Evidence for an extended scattered disk.

B. Gladman[1], M. Holman[2], T. Grav[3],
J. Kavelaars[4], P. Nicholson[5], K. Aksnes[3], J-M. Petit[1]

[1]Observatoire de la Côte d'Azur, France
[2]Harvard-Smithsonian Center for Astrophysics, USA
[3]University of Oslo, Norway
[4]McMaster University, Canada
[5]Cornell University, USA

Proposed running head: Evidence for an extended scattered disk.

Re-submitted to Icarus, Jan 28/2001

Keywords: Kuiper belt objects; trans-neptunian objects; comets, dynamics.

29 text pages + 6 figures + 2 tables = 37 pages in revised submission

Abstract

By telescopic tracking, we have established that the trans-neptunian object (TNO) 2000 CR_{105} has a semimajor axis of 220±1 AU and perihelion distance of 44.14±0.02 AU, beyond the domain which has heretofore been associated with the 'scattered disk' of Kuiper Belt objects interacting via gravitational encounters with Neptune. We have also firmly established that the TNO 1999 TL_8 has a high perihelion (of 40.08±0.02 AU). These objects, and two other recent discoveries which appear to have perihelia outside 40 AU, have probably been placed on these orbits by a gravitational interaction which is *not* strong gravitational scattering off of any of the giant planets on their current orbits. Their existence may thus have profound cosmogonic implications for our understanding of the formation of the outer Solar System. We discuss some viable scenarios which could have produced these objects, including long-term diffusive chaos and scattering off of other massive bodies in the outer Solar System.

This discovery implies that there must be a large population of TNOs in an 'extended scattered disk' with perihelia above the previously-suggested 38 AU boundary. The total population is difficult to estimate due to the ease with which such objects would have been lost. This illustrates the great value of frequent and well time-sampled recovery observations of trans-neptunian objects within their discovery opposition.

1 Introduction

Current nomenclature commonly divides the trans-neptunian region of the solar system into the 'Kuiper Belt' (consisting of so-called 'classical belt' objects and 'resonant objects' in various mean-motion resonances with Neptune), and the 'scattered disk' (Jewitt *et al.* 1998). Finer distinctions and sub-populations are possible (see Gladman *et al.* 2001). The 'scattered disk' is a structure that was observed to form naturally in simulations of orbital perturbation of comets exterior to Neptune (Torbett and Smoluchowski 1990) and of the delivery of Jupiter-family comets from the Kuiper Belt (Duncan and Levison, 1997). The first recognized member of this population of scattered disk objects (SDOs) was 1996 TL_{66} (Luu *et al.* 1997); since that time of order 40 have been identified (*cf.*, Trujillo *et al.* 2000), with orbital determinations of varying quality.

In studies of dynamical chaos in the trans-Neptunian region Torbett and Smoluchowski (1990) realized that many objects with chaotic dynamics outside 30 AU would eventually encounter Neptune and be dispersed into a large scattered disk, but they did not examine the dynamics of these objects in detail. While studying the transport of Jupiter-family comets towards the Sun from a putative Kuiper Belt source, Duncan and Levison (1997) showed that as trans-neptunian objects (TNOs) leave the Kuiper Belt after encountering Neptune, some are scattered outward to large, long-lived external orbits rather than being passed inward to the other giant planets; they also calculated the steady-state orbital distribution of this material. They showed that high-order orbital resonances could temporarily raise orbital perihelia and thus temporarily 'decouple' some of these objects from Neptune. Because these groups of dynamicists observed this structure's creation via gravitational scatterings with Neptune, the term 'scattered disk' arose.

Once on scattered orbits, the SDO population dynamically eroded as SDOs are eventually perturbed by Neptune back onto orbits geometrically crossing that planet's orbit. Then they are eventually ejected by Neptune, or have their perihelia pushed interior to the orbit of Uranus at which point their dynamical lifetimes become $\sim$10 Myr, usually being rapidly ejected from the Solar System (Dones *et al.* 1996, 1997, Levison and Duncan 1997). Objects scattered to large orbits by Neptune will return to near the planet at subsequent perihelion passages. For a scattered object the gravitational perturbation from Neptune might be considered as an impulse as the object passes its perihelion; this alters the velocity of the object but not its position. Thus, the q's of scattered objects generally remain small, maintaining the possibility of encounters with the planet. Nevertheless, the state with $q > 30$ AU but still near Neptune can be very long-lived due to the large orbital periods and the low probability of Neptune being nearby when the object's rapid perihelion passage occurs.

Levison and Duncan (1997, Fig. 6) show that except for some cases in the 2:1 resonance with $a \simeq 48\ AU$, objects with $q >$40 AU are entirely absent or at least are of extremely low probability. Some objects have their perihelia raised from 35 to $\sim$38 AU due to a phenomena of 'resonance sticking', to which we will return. Torbett (1989) and Torbett and Smoluchowski (1990) explored the dynamics of large-a orbits with q near Neptune. They showed that such orbits (up to $q \simeq$45 AU) could be dynamically chaotic for large semimajor axes. Although exhibiting chaotic evolution does not guarantee orbital instability (*cf.* Gladman 1993), it was later seen to be strongly correlated with it in long-term numerical integrations in the regime of common exploration (out to about a=50 AU, Duncan *et al.* 1995). However, the *time scale* for orbital instability may be very long; a chaotic orbit at high a and high q may require >5 Gyr to reach a state where it begins to interact strongly with Neptune.

There is as yet no firm definition of the boundaries of the SDO population. That is, there is no clear definition of what separates the SDOs from the Centaurs, nor the SDOs from the rest of the Kuiper Belt (Gladman 2001), although the perihelion distance is often used to separate the populations. Trujillo *et al.* (2000) seem to *define* the SDO population as that with q=34–36 AU. Based on their simulations, Duncan and Levison (1997) adopted q=30–40 AU and $a > 50$ AU, although there seems to be no reason to exclude $q < 30$ AU. The semimajor axis, a, distribution of these objects has no formal upper limit in the simulations of Duncan and Levison (1997), although a distinction from the inner Oort cloud becomes problematic at $a > 1000$ AU (Duncan *et al.* 1987). The currently-known SDOs (Fig. 1) must be more concentrated towards lower a than the 'real' distribution due to selection biases; larger-a SDOs spend smaller fractions of their time near perihelion where they appear brightest and are more easily detected. A bias towards small perihelion distance q will also exist.

In this paper we describe observational work which has detected the first members of a population of TNOs whose perihelia are outside of 40 AU, beyond the domain which has heretofore been associated with the 'scattered disk' of Kuiper Belt objects interacting via gravitational encounters with Neptune. Given the biases against discovering and determining the orbits of such objects, we argue that their existence implies a very large population which may rival or exceed that of the 'known' Kuiper Belt. We will discuss how this population may have arisen.

2 Observations

In order to appreciate the complications inherent in tracking and estimating the population of objects with large semimajor axes, we explain in some detail the observational history of the objects whose orbits are discussed in this paper.

The object 2000 CR_{105} was discovered on 6 February 2000 in an on-going survey by Millis *et al.* (2000), and, based on the observed 3-week arc from a second night's observations on 27 February, the Minor Planet Center (MPC) placed it on a provisional 'scattered orbit' with a=82 AU, e=0.59, and i=31°, implying q=33.8 AU. The semimajor axis was chosen to be similar to that of 1996 TL_{66} (B. Marsden, 2000, private communication). Since the estimated heliocentric distance at the time of discovery was $\simeq$55 AU, we realized this object was potentially of exceptional interest; only the much fainter 1999 DG_8 (Gladman *et al.* 2001), at 62 AU, had ever been discovered at such a large heliocentric distance. Thus, we re-observed 2000 CR_{105} on 28 and 29 March 2000 at the Canada-France Hawaii 3.5-m telescope; given the short time interval since the previous observation, we were stunned to find the object already a dramatic 24 arcseconds off the ephemeris — an enormous positional error for a trans-neptunian object. This implied that the object was moving eastward much more rapidly than indicated by the initial orbit and thus had a much larger semimajor axis. Based on these observations, the orbit was revised by B. Marsden to a=675 AU, e=0.94, i=23°, making it the largest scattered disk orbit known at that time. Even with this preliminary orbit the perihelion (q=41 AU) had risen out of the region believed to be strongly coupled to Neptune, but given a two-month arc on an orbital period of greater than 10,000 years, this perihelion distance was still rather uncertain. A further recovery attempt by M. Holman *et al.* in May 2000 at Kitt Peak failed in bad weather, after which 2000 CR_{105} disappered behind the Sun until November 2000.

At this point there was a broad range of possible orbits for 2000 CR_{105}. Its astrometry was still formally consistent, within observational errors, with a parabolic orbit corresponding to a returning Oort cloud comet (albeit with the most distant perihelion ever observed). There was even the possibility that the orbit was hyperbolic (corresponding to the first observed interstellar comet), although this was less likely. It was still possible that CR_{105} would turn out to have q <39 AU and a relatively 'typical' scattered disk orbit, but with a large semimajor axis. Lastly, and most interestingly, if a q >40 AU perihelion could be confirmed then, we believed at the time, this object would turn out to be the first SDO beyond the dynamical influence of the giant planet system.

We thus decided to allocate considerable telescope time to the recovery and orbit determination of this object, beginning in the dark run of November 2000 and continuing every dark run until February 2001, to provide a high-quality data set on which to base orbital fitting. By March 2001 the unique orbit of this object was secure. Table 2 summarizes these efforts, along with the third-opposition recovery at the Nordic Optical Telescope. Note the frequent time sampling in the second (recovery) opposition and the abundance of observations away from opposition, which helps reduces the uncertainty in the orbital elements (Bernstein and Khushalani 2000). It is worth noting that without our March 2000 observations this object would have been 19 arcminutes away from its original ephemeris one year after discovery and would likely not have been recovered without considerable effort, even with the mosaic camera on which it was discovered. Based on this experience, it seems very plausible that some of the TNOs with only short arcs in their discovery opposition and then not found at their second opposition may very well have orbits similar to that of 2000 CR_{105}. We thus take a fraction of 1 in ~500 known TNO orbits as a lower limit to the number of 2000 CR_{105}-like objects that have been detected in the flux-limited TNO/SDO database.

Based on it's apparent R-band magnitude of $m_R = 23.3 \pm 0.5$, and an assumed 4% albedo, 2000 CR_{105}'s diameter is roughly 400 km. We do not consider the photometric data reliable enough, nor the assumed albedo accurate enough, to believe this to be accurate to more than a factor of two (2-sigma). This size places 2000 CR_{105} at the high end of the known size range of trans-neptunian objects, a factor of 2–3 below the largest known objects.

The second TNO with a known high perihelion is 1995 TL_8, an object discovered by the Spacewatch program (Larsen *et al.* 2001). It had a much smaller semimajor axis ($a \simeq$59 AU), but also appeared to have a perihelion above 40 AU. We tracked this object in February 2001 (at the Nordic Optical Telescope) and August 2001 (from the Calar Alto 2-meter). These observations confirmed that this object has $q >$40 AU and that it is potentially near a 4th order mean-motion resonance with Neptune (see below).

The TNO 2000 PH_{30}, discovered and tracked to its 2001 opposition by our group, has $q \sim$40 AU, and the TNO 2000 YW_{134} = 2001 XG_{201} (Minor Planet Electronic Circular 2002-A26) has recently been established as another high-q TNO ($q \simeq$41.4 AU). Because these last two objects have only 2-opposition orbits, their pericentric distances are less well constrained and we will not draw strong conclusions below from their currently uncertain orbits.

3 Orbit modelling

Using the available astrometric data, we have computed an osculating orbit solution taking into account the perturbations of the 4 giant planets (Table 1), using the orbit determination software of Bernstein and Khushalani (2000), optimized specifically for outer Solar System objects. This algorithm provides error estimates in the fitted osculating orbital elements (Table 2).

Based on the available data, 2000 CR_{105}'s orbit is large, highly elliptical, and moderately inclined (Table 2). 2000 CR_{105} is currently 53 AU from the Sun and moving outwards, having passed perihelion in mid-1965. At perihelion the object would have been about 0.8 magnitudes brighter. The mean anomaly, argument of perihelion, and longtiude of node are all well-determined. Overall this TNO might look like an outlier in the scattered disk distribution except for its very high q =44 AU perihelion (see Fig. 1). The perihelion distance has a fractional uncertainty much smaller than a because a and e are strongly correlated; the uncertainty in the perihelion distance is only ~0.1%.

It is 2000 CR_{105}'s exceptionally large perihelion distance which merits special attention

(Figure 1). This figure shows that the only other TNO with perihelion sure to be above 40 AU is 1995 TL_8, whose most recent published orbit from the Minor Planet Center is (a, e, i)=(52.78,0.24,0.20°). (Note that the MPC orbits are given in heliocentric osculating elements). 1995 TL_8 is near the 3:7 mean-motion resonance with Neptune (A. Morbidelli and D. Nesvorny, private communication 2001), which might thus be involved in raising the object's perihelion.

4 Cosmogonic implications

In this section we wish to discuss possible scenarios for how 2000 CR_{105} and other high-q TNOs arrived on their current orbit. These include perihelion raising by diffusive chaos, as well as scattering due to (1) now-absent primordial embryos which passed through the forming Kuiper Belt, (2) a young Neptune that was forming a 'fossilized scattered disk', (3) an unknown resident planetary-scale object in the distant Kuiper Belt, or (4) passing stars. Because CR_{105} turns out to be the most difficult case, we will base much of our discussion on this object.

4.1 Diffusive chaos

We conducted a variety of numerical experiments to investigate the long-term dynamics of 2000 CR_{105}. We first numerically integrated the best-fit orbit of this object, along with 20 other sets of initial conditions distributed consistent with the estimated errors in the orbital elements; these initial conditions cover the entire region (>3-sigma) of the 3-opposition orbit. 2000 CR_{105} and its "clones" were modelled as test particles moving in the gravitational field of the giant planets. The planetary positions and velocities came from the JPL DE403 ephemeris (with the terrestrial masses added to the Sun). The symplectic n-body map of Wisdom and Holman (1991) was used with a time step of 0.5 year for 5 Gyr of simulated time.

In addition to following the object trajectories, the tangent equations for each trajectory were also integrated (Holman and Murray 1996, Mikkola and Innanen 1999), allowing us to estimate the rate at which nearby trajectories diverge from each other. Regular or quasi-periodic trajectories separate from each other linearly or at most polynomially with time. Chaotic motion is characterized by exponential divergence of neighboring trajectories; the time scale of this divergence is called the Lyapunov time.

All of the trajectories share a number of characteristics: (1) Each is chaotic with a Lyapunov time from 5×10^4 to 10^5 years (15 to 30 orbital periods), consistent with previous studies of objects in this a, e regime (Torbett 1989, Torbett and Smoluchowski 1990). (2) the semimajor axis oscillates rapidly within a series of discrete ranges. (3) The eccentricity also varies rapidly; however, this variation is correlated with a in such a way that q varies much more smoothly. This occurs because the object receives an impulsive kick from Neptune as it passes perihelion; at each conjunction the position or perihelion distance of the object is nearly unaltered but the velocity, and thus a and e, is changed.

Malyshkin and Tremaine (1999) developed a 2-dimensional "keplerian map", based on the planar restricted three-body problem, to study the long-term evolution of eccentric comet orbits perturbed by Neptune. Although their mapping assumes a fixed q and models the entire interaction as an impulsive kick at perihelion passage, their results capture many of the features seen in our integrations. Two of their principle results are: (1) the phase space is densely covered with chains of islands from mean-motion resonances, and (2) the chaotic zone between these islands is contiguous. That is, a trajectory can diffuse to arbitrarily large semimajor axis.

Fig. 2 shows a typical example of the evolution of a and q. The rapid $\sim$50 Myr oscillation of q is caused by the "Kozai effect" of Neptune on the test particle (Kozai 1962), but its amplitude is far too low (see Thomas and Morbidelli 1996) to bring q down to small values. The center of each of the a-ranges, around which rapid oscillations occur, corresponds to a high-order mean-motion resonance with Neptune. This demonstrates the so-called phenomenon of "resonance sticking" in which chaotic trajectories are trapped, for possibly extended periods, near the boundaries of a resonant island (Karney 1983, Meiss 1992). This resonance sticking proves that 2000 CR_{105} is in or near a regime in which chaotic phenomena are operating and that this region of phase space may be connected to regions of lower perihelion by an extended chaotic zone; this suggests the *possibility* that 2000 CR_{105} was on a more 'typical' SDO orbit which then diffused via chaotic phenomena to its current high perihelion state.

The long time-scale variations of perhelion distance are important for evaluating the plausibility of this hypothesis. Of the 20 integrated particles, 2 diffused to minimum q's of 39 AU at some point during their integrations, although most remained between 42 and 47 AU (Fig. 3). We extended the integration of a test particle to determine the long-term fate of this object; the "random walk" in q continued, with a maximum observed perihelion distance of $q = 50$ AU. An orbit with $q \sim 40$ AU was attained after 24 Gyr, at which point the semimajor axis diffused to very large (10^3 AU) values; shortly thereafter q dropped even lower and the particle was ejected from the Solar System by Neptune. The integrations demonstrate that particles in the orbital region of 2000 CR_{105} can, over very long time scales, reach perihelion distances at which strong scatterings due to Neptune occur. Of course, the opposite can occur because the equations of motion are time-reversible. The fact that none of the clones reached q=35 AU on 5 Gyr time scales indicates that the probability of the reversed process of reaching the current state of 2000 CR_{105} is low. In particular, the probability of leaving the vast chaotic zone to enter the slowly-diffusing regime is unconstrained; the absence of such trajectories in the Levison and Duncan (1997) simulations implies it is low.

To determine the origin of the observed dynamical chaos, we extended the work of Torbett and Smoluchowski (1990) by integrating 5400 test particles trajectories with q=30–52 AU for 10^8 years (Fig. 4). We estimated the Lyapunov time of each trajectory. In Fig. 1 we plot a point at those values of a and q for which the corresponding trajectory was chaotic with a Lyapunov time less than 10^5 years. (As a test we checked that our high-e test particles, when integrated without planetary perturbations, were not chaotic.) Based on earlier descriptions of the boundaries of the scattered disk, we expected to see chaos for trajectories with q below a fixed value (a horizontal dividing line); our results show that SDOs with large a can have large q and still exhibit chaos on orbital-period time scales.

To understand the time scale of this chaos, we compared the Lyapunov times of the particles to their orbital period and found that a value of 20 test-particle orbital periods separates those trajectories that are strongly chaotic from those that are not. For large semimajor axix, using the orbital period of the test particle itself is probably the best reference time scale. In Fig. 4 we plot the initial a and e of those trajectories with non-zero Lyapunov times, both longer (points) and shorter (open squares) than 20 orbital periods. The solid line is a rough empirical estimate for the envelope of the trajectories chaotic on time scales of <20 orbital periods; few trajectories chaotic on 'orbital-period time scales' are found below the line. Below the line some 'weak chaos' is found which functions on time scales much longer than the orbital period. The narrow 'fingers' of non-chaotic trajectories that extend above the line correspond to the stable islands of high-order mean-motion resonances with Neptune. These resonances are narrow but not microscopically so; at high e resonance widths do not depend as strongly on the order of the resonance as they do at low eccenticity. An analytic estimate of the width of the 6:1 mean motion resonance with Neptune, for example, yields roughly 3 AU at Neptune-crossing eccentricity (Morbidelli *et al.* 1995). On either side of these 'fingers' are chaotic regions resulting from the *overlap* of adjacent resonances. A detailed resonance overlap calculation, extending the work of Wisdom (1980), can be completed at high eccentricity by employing the technique of Ferraz-Mello and Sato (1989).

We briefly note that the TNO 1995 TL_8 is near a region which might plausibly be reached by chaotic diffusion related to the nearby 3:7 mean-motion resonance. If the estimated q=41.4 of 2000 YW134 is confirmed, its somewhat higher perihelion may pose a greater problem, although the 3:8 mean-motion resonance with Neptune is nearby.

Finally, to address the probability of insertion of scattered TNOs into extended scattered disk orbits, we have extended the integrations of Guillot and Gladman (2001), who studied the fates of 10,000 test particles which started between 4 and 40 AU to study late planetesimal accretion by the giant planets. During the first 100 Myr of these simulation, no particles were observed to reach q >40. We extended the integration of 3000 of their initial conditions to 1 Gyr, and of another 7000 to 400 Myr to see if on this longer time scale perihelion-raising could occur. As in Duncan and Levison (1997), perihelion lifting was seen to occur inside mean-motion resonances with Neptune, especially the 2:1 (*cf.* Levision and Duncan 1997). Fig. 5 shows an example of this process. However, none of the integrated trajectories with $a > 100$ AU ever exhibited $q > 38$ AU, and for a=50–100 AU this only occurred temporarily for $\sim 0.1\%$ of the particles, and then only inside low-order mean-motion resonances. Fig. 6 presents a magnification of the region near 2000 CR_{105} showing the region traversed by test particles during the 1 Gyr integrations; no particles were observed to rise above q=37 AU. In the more extensive integrations of Levison and Duncan (1997) some additional phase space up to nearly q=38 AU is accessed (H. Levison and L. Dones, private communication 2001). We conclude on the basis of these integrations that the probabililty of reaching a dynamical state like that of 2000 CR_{105} from a set of dynamically 'cold' (with low initial i in particular) is less than 1 in 10^3. The likelihood of reaching a dynamic state like that of CR_{105} may be higher if initial conditions with larger inclinations are used (Dones 2001, private communication).

The details of our discussion are best refined once the semimajor axis uncertainty of 2000 CR_{105} drops below 0.1 AU, allowing us to determine exactly where in phase space it resides; it could conceivably be in a dynamically more stable region. Although we have given an extensive discussion of the diffusive chaos hypothesis (due to the fact that we can easily explore it numerically), the cosmogonic implications are even more dramatic if this hypothesis is either incorrect or untenable due to low probability. In such a case the existence of objects weakly coupled to the planetary system provides strong constraints on the formation of the outer Kuiper Belt. We now discuss three scenarios which could produce large numbers of such weakly-coupled or decoupled TNOs.

4.2 Primordial Embryos

Given that 4 planets with masses greater than 10 Earth masses formed in the outer Solar System, it is unlikely that no objects with martian-terrestrial mass also formed in the region. Morbidelli and Valsecchi (1997) and Petit *et al.* (2000) developed the idea that one or several of these objects (which they call 'embryos') would have been logically scattered outward by Neptune and spent some time as SDOs transiting the forming Kuiper Belt, thus causing the dynamical excitation and mass loss observed therein. Close encounters with these passing embryos disturb the Kuiper belt out to the aphelic distance of the embryos, which are often 50-100 AU; scattering events can thus produce TNOs with perihelia well past Neptune on high-e orbits. Once the embryos are eliminated by further gravitational interactions with Neptune, as 90% of SDOs are in 10 Myr (Duncan and Levison 1997), the TNOs remaining are extremely long-lived. In this scenario 2000 CR_{105} may represent an object formed outside 50 AU which was scattered to a large-e orbit due to encounters with one of these embryos. Perhaps more likely, 2000 CR_{105} could have been formed much closer and *also* became a SDO via scattering by Neptune and then an encounter with a distant embryo sufficed to raise q to 44 AU.

4.3 Fossilized scattered disk

Thommes *et al.* (1999) propose that the 'embryo' passing through the Kuiper Belt may have been Neptune itself, during a formation process in which it transited the Kuiper belt on an orbit either more eccentric or with larger a before reaching its present nearly circular orbit at 30 AU. Being much more massive than the embryos discussed above, Neptune would be able to produce extensive dynamical 'damage' in a shorter time. With its current a and a modest e of $\sim$0.3, which Thommes *et al.* damp via gravitational friction with a massive planetesimal disk in the vicinity, Neptune's could encounter particles as far out as 44 AU. After Neptune's aphelion evolves out of the 40 AU region (presumably rapidly) the TNOs with q above this limit are 'fossilized' on orbits which either do not evolve over the lifetime of the solar system, or evolve only slowly via the diffusive mechanisms discussed above. 2000 CR_{105} could be an example of the latter case.

4.4 Resident planet

Another possibility is that 2000 CR_{105} arrived in its current dynamical state due to gravitational interaction with a planetary-sized body that is *still resident* in the Kuiper Belt. This could come about in two ways. First, in the distant Kuiper belt, beyond the region sculpted by the whatever processes disturbed the 30-50 AU region, a planetary-mass body (the size of the moon to Mars for example), or several, may have formed *in situ* over the lifetime of the solar system and the perturbations of this body have sculpted the outer Kuiper belt. A Mars-sized body (with escape velocity of 5 km/s) at 100 AU where orbital velocities are only $\sim$ 3 km/s could scatter a body like 2000 CR_{105} to its present orbit.

More likely may be a scenario in which several lunar—martian mass bodies were in the scattered disk, traversing the 50–200 AU region. Many such bodies were likely formed interior to Neptune as the cores of the giant planets were accreting, and some would have ended up as SDOs. Since orbital velocities at those distances are comparable to the escape speeds of these bodies, mutual encounters between the 'embryos' could place one or more of them on orbits entirely exterior to Neptune; the planetary embryos still coupled to Neptune would have been rapidly ejected, leaving the decoupled embryo(s) 'lodged' in the distant Kuiper belt. The resident embryo would then perturb the orbital distribution, of the scattered disk. Similar ideas trace back to Fernández (1980) and Ip (1989), who sought to push short-period comets to Neptune-crossing orbits via decoupled embryos before long-term gravitational erosion was characterized as a supply process (Levison and Duncan 1997). Unpublished simulations by Morbidelli (2000, private communication) and Brunini *et al.* (1999, private communication; Icarus, submitted 2001) show that this decoupling process can happen naturally. This scenario could be responsible for the apparent lack of objects on nearly circular orbits outside the 2:1 resonance (see Jewitt *et al.* 1998, Allen *et al.* 2000, and Gladman *et al.* 2001 for discussion) and the lack of detection of the so-called 'Kuiper Wall' (Trujillo 2000).

4.5 Passing Stars

A last scenario is that high-pehihelion orbits have been produced due to the close passage of another star. Ida et al. (2000) show that a very close passage could perturb the Kuiper belt and raise a particle with a ~200 AU from a circular orbit to one like that of CR_{105}; building such a large object at that distance when our young Sun may have been in a dense stellar environment (in order to have a non-negligible probablility for such a close passage) may be problematic. However, Fernandez and Brunini (2000) showed that objects already emplaced in the scattered disk could suffer orbital perturbations due to more distant stellar passages sufficient to raise their perihelia.

5 Discussion

Having examined the possibility that diffusive chaos might produce the orbits of these objects and briefly discussed other cosmogonic possibilities, we turn to the ramifications of the identification of this population.

The importance of these high-q objects is related to the large population implied due to their relative unobservability. Extremely roughly, we estimate that the majority of the TNO surveys to date, having searched of order 300 square degrees within $\sim 5°$ of the ecliptic to limiting magnitude m_R=23–24, are capable of detecting 2000 CR_{105} for only a small fraction of its orbital period. A simple Monte-Carlo simulation shows that the 400-km diameter 2000 CR_{105} brightens above m_R=23–24 near perihelion for only 1–2% of its orbital period; accounting for the fraction of time an object with a 23° orbital inclination spends within 5° reduces it to being visible for only ~0.1–0.3% of the time in the previous surveys. Estimating that these objects are spread over the sky within ±30° of the ecliptic (about $2{\times}10^4$ square degrees) implies a lower limit of $\sim 10^4$ such objects (because other objects already detected within the surveyed region of the sky may have in fact had high q and been lost). Objects with perihelion higher than 44 AU would be even harder to detect and identify via orbital tracking. Given this extreme detection bias against finding objects like 2000 CR_{105}, there must be a large number of objects with perihelia higher than the 34–38 AU range previously defined for the scattered disk. Taking a power-law cumulative size distribution with index of roughly 3 implies a population of $\sim 10^4 \times 4^3 \sim 10^6$ objects with diameter larger than 100 km, 1-2 orders of magnitude larger than the previously-estimated populations of 'classical' Kuiper Belt between 30 and 50

AU (Jewitt et al 1998) and the scattered disk (Trujillo et al 2000).

Thus, the 'scattered disk' of objects currently strongly coupled to Neptune may merge into a much more massive 'extended scattered disk' where objects are only weakly perturbed by Neptune. We take the above estimates as good to only 1–2 orders of magnitude, implying that the extended scattered disk population at least rivals the previously-known components of the Kuiper Belt.

We propose that for the moment these objects should *not* be classified as scattered disk objects unless a definition can be arrived at which would delineate SDOs from an object on a regular orbit (for example, a=210 and e=0.7, which is neither chaotic nor coupled to Neptune) and yet clearly not a member of a primordial 'cold disk' of low-e and low-i planetesimals. If the eccentricity and inclination distribution of the extended scattered disk does not have the structure of a fossilized disk (with a gap in eccentricity between the high-e scattered particles and much lower e primordial particles) then it will be difficult to say where the 'extended scattered disk' ends! These nomenclature problems are expanded upon in Gladman (2002).

We are not yet able to reliably estimate the likelihood that these large-q objects have diffused to their $q > 40$ AU orbits after emplacement in the regular scattered disk. The rarity of such particles in our integrations and those of Levison and Duncan (1997) indicates that this is roughly <1 in 10^3 of the SDOs initially populating the scattered disk. The number of SDOs currently remaining in this $q < 40$ AU scattered disk (3×10^4 with diameters D >100 km, Trujillo *et al.* 2000) is estimated to be 1% of the initial population (Duncan and Levison 1997), implying an initial population of 3×10^6 SDOs with D >100 km. If the extended scattered disk currently contains $\sim 10^6$ objects such objects (whose orbits are essentially stable over 4.5 Gyr) then this implies an emplacement efficiency of 30%, which we believe the dynamical simulations rule out. If, on the other hand, 2000 CR_{105} is a 'lucky find of a big object' and the extended disk contains only $\sim 10^4$ object with D >100 km, then only 1 in $\sim$ 300 initial SDOs need to reach the high-q state to give a current fraction of 1/3 and dynamical diffusion may be a practical solution. To disprove this hypothesis would require the direct integration of $\sim 10^4 - 10^5$ particles initially in the scattered disk to show that the emplacement efficiency via only diffusion is firmly below 1 in 10^3. The effect of the initial inclination distribution of particles which are fed into the scattered disk from the giant planet regime should be studied.

Given the direct detection bias against, and the possible earlier loss of other already-discovered objects that may have been on similar orbits, the actual fraction of the visible trans-neptunian region that is also on high-q orbits could be as large as several percent of the designated objects (currently 2–4 exist, depending on what definition is used and how reliable the orbits of 2000 PH_{30} and 2000 YW_{134} are). In this case the diffusive hypothesis may become untenable and some of the more cosmogonically dramatic scenarios may be necessary. If a high-a TNO totally decoupled from the planetary system can be identified then the reality of these dramatic scenarios can be constrained; the fact that the first high-q TNOs are in the diffusive boundary regime would then be understood to be due to detection bias which favors the latter's discovery. One cannot stress enough that continued tracking of *all* discovered TNOs, especially 2–3 months after discovery and then into the second opposition, is necessary in order to reliably estimate the fraction of the Kuiper Belt that is in the extended scattered disk.

6 Conclusion

The observational limits on the population of extended scattered disk objects are weak, because high-a objects which pass with perihelia well above 40 AU are only bright enough to be seen for a small fraction of their orbital period. This structure may extend the 'scattered disk' out to very great distances. A model of the extended scattered disk is premature since a population estimate coming from such a model would depend entirely on the assumed q distribution. More observations are required to improve our knowledge of the distant Kuiper Belt; the identification of several more would prove that this population rivals that of the entire Kuiper belt and 'regular' scattered disk.

The lesson provided by our tracking of the exceptional TNO 2000 CR_{105} is that follow up inside the first year (2–3 months after discovery) is critical in order to detect these large orbits, for without such a recovery the TNO will be very far from even a 'normal' scattered orbit one year later, at which point recovery becomes problematic without the expense of considerable observations resources. Our knowledge of the dynamical structure of the outer Solar System need not be limited by the assumptions imposed by the lack of reliable tracking of the detected objects. The preferential loss of the most exceptional trans-neptunian objects warps our view of the Kuiper Belt.

7 Acknowledgements

B. Gladman, J. Kavelaars, and M. Holman were visiting astronomers at the Canada France Hawaii telescope, operated by the National Research Council of Canada, le Centre National de la Recherche Scientifique de France, and the University of Hawaii. Data from VLT collected at the European Southern Observatory, Chile, proposals 66.C-0048A and 66.C-0029A. Observations at the Palomar Observatory were made as part of a continuing collaborative agreement between the California Institue of Technology and Cornell University.

K. Aksnes, T. Grav, and M. Holman were visiting astronomers at the Nordic Optical Telescope. The Nordic Optical Telescope is operated on the island of La Palma jointly by Denmark, Finland, Iceland, Norway, and Sweden, in the Spanish Observatorio del Roque de los Muchachos of the Instituto de Astrofisica de Canarias. Some of the data presented here have been taken using ALFOSC, which is owned by the Instituto de Astrofisica de Andalucia (IAA) and operated at the Nordic Optical Telescope under agreement between IAA and the NBIfAFG of the Astronomical Observatory of Copenhagen.

M. Holman, B. Gladman, and T. Grav were visiting astronomers at the Kitt Peak National Observatory, National Optical Astronomy Observatory, which is operated by the Association of Universities for Research in Astronomy, Inc. (AURA) under cooperative agreement with the National Science Foundation.

J-M. Petit was a visiting astronomer at the Calar Alto observatory.

This work was supported in part by an ACI Jeune grant from the French Ministry of Research, and NASA grants NAG5-10365 and NAG5-9678 to the Smithsonian Astrophysical Observatory (SAO). T. Grav is supported by an SAO Predoctoral Fellowship. We thank Joe Burns, Brian Marsden, Alessandro Morbidelli, and Norm Murray for helpful input.

References

Allen, L., Bernstein, G., and Malhotra, R. 2001. The edge of the solar system. *Ap. J. Lett.* **549**, 241–244.

Bernstein, G. and Khushalani, B. 2000. Orbit Fitting and Uncertainties for Kuiper Belt Objects. *A. J.* **120**, 3323-3332.

Dones, L., H. F. Levison, and M. Duncan 1996. On the dynamical lifetimes of planet-crossing objects. In *Completing the Inventory of the Solar System* (T. W. Rettig, J. Hahn Eds.), Astronomical Society of the Pacific Press, Vol. 107, pp. 233–244.

Dones, L., Gladman, B., Melosh, H. J., Tonks, W. B., Levison, Harold F., Duncan, M. 1997. Dynamical Lifetimes and Final Fates of Small Bodies: Orbit Integrations vs Opik Calculations. *Icarus* **142**, 509-524.

Duncan, M., Quinn, T., Tremaine, S. 1987. The formation and extent of the solar system comet cloud. *A. J.* **94**, 1330-1338.

Duncan, M. J., Levison, H. F. (1997) A scattered comet disk and the origin of Jupiter family comets. *Science* **276**, 1670-1672.

Fernandez, J.A., and Brunini, A. 2000. The buildup of a tightly bound comet cloud around an early Sun immersed in a dense galactic environment: Numerical experiments. *Icarus* **145**, 580-590.

Ferraz-Mello, S., Sato, M. 1989. The very-high-eccentricity asymmetric expansion of the disturbing function near resonances of any order. Astronomy and Astrophysics **225**, 541–547.

Gladman, B. 1993. Dynamics of systems of two close planets. *Icarus* **106**, 247-263.

Gladman, B. 2002. Nomenclature in Kuiper Belt, in *Proceedings of Joint Discussion 4 of the 2000 IAU General Assembly.* (A. Lemaitre Ed.) Kluwer, in press.

Gladman, B., Kavelaars, J., Petit, J-M., Morbidell, A., Holman, M., Loredo, T. 2001. The Structure of the Kuiper Belt: Size Distribution and Radial Extent. *Astron. J.* **122**, 1051-1066.

Guillot, T., and Gladman, B. 2001. in *Disks, Planetesimals and Planets: ASP conference series Vol. 219*, (F. Garzón *et al.* Eds.), 475–485.

Ip, W.-H. 1989. Dynamical processes of macro-accretion of Uranus and Neptune - A first look. *Icarus* **80**, 167-178.

Jewitt, D. G., Luu, J., and Chen, J. 1996. The Mauna Kea-Cerro-Tololo Kuiper Belt and Centaur Survey. *A. J.* **112**, 1225-1238.

Jewitt, D. G., Luu, J., and Trujillo, C. 1998. Large Kuiper Belt objects: The Mauna Kea 8K CCD survey. *A. J.* **115**, 2125-2135.

Karney, C. F. F. 1983. Long-term correlations in the stochastic regime. *Physica* **8D**, 360-380.

Kozai, Y. 1962. ecular perturbations of asteroids with high inclination and eccentricity.

Astron. J. **67**, 591-598.

Larsen, J. A., Gleason, A. E., Danzl, N. M., Descour, A. S., McMillan, R. S.; Gehrels, T., Jedicke, R., Montani, J. L., Scotti, J. V. 2001. The Spacewatch Wide-Area Survey for Bright Centaurs and Trans-Neptunian Objects. *Astron. J.* **121**, 562-579.

Levison, H. F., Duncan, M. J. 1997. From the Kuiper Belt to Jupiter-Family Comets: The Spatial Distribution of Ecliptic Comets. *Icarus* **127**, 13-32.

Malyshkin, L., Tremaine, S. 1999. The Keplerian Map for the Planar Restricted Three-Body Problem as a Model of Comet Evolution. *Icarus* **141**, 341–353.

Meiss, J. D. 1992. Symplectic maps, variational principles, and transport. *Rev. Mod. Phys.* **64**, 795-848.

Mikkola, S., Innanen, K. 1999. Symplectic Tangent map for Planetary Motions *Celest. Mech. Dyn. Astron.* **74**, 59–67.

Millis, R. L., Buie, M. W., Wasserman, L. H., Elliot, J. L., Kern, S. D., Wagner, R. M. 2000. The Deep Ecliptic Survey. *B.A.A.S.* **32**, 1028–1029.

Morbidelli, A., Thomas, F., Moons, M. 1995. The resonant structure of the Kuiper belt and the dynamics of the first five trans-Neptunian objects. Icarus, **118**, 322–340.

Morbidelli, A. and Valsecchi, G. 1997, NOTE: Neptune Scattered Planetesimals Could Have Sculpted the Primordial Edgeworth-Kuiper Belt. Icarus, **128**, 464.

Petit, J-M., Morbidelli, A. and Valsecchi, G. 1999. Large Scattered Planetesimals and the Excitation of the Small Body Belts. Icarus, **141**, 367.

Torbett, M. 1989. Chaotic motion in a comet disk beyond Neptune: The delivery of short-period comets. A.J. **98** 1477-1481.

Torbett, M. and Smoluchowski, R. 1990. Chaotic motion in a primordial comet disk beyond Neptune and comet inlux to the solar system. Nature, **345**, 49–51.

Thomas, F., and A. Morbidelli (1996) The Kozai resonance in the outer solar system and the dynamics of long–period comets Celest. Mech., **64**, 209–229.

Thommes, E., Duncan, M., Levison, H.F. 1999. The formation of Uranus and Neptune in the Jupiter-Saturn region of the Solar System. Nature, **402**, 635–638.

Trujillo, C. 2000. Simulations of the bias effects in Kuiper Belt surveys. in *Minor Bodies in the Outer Solar System* (A. Fitzsimmons, D. Jewitt, R.M. West, Eds.) pp. 109–115. Springer-Verlag, Berlin.

Trujillo, C., D. Jewitt, Luu, J. 2000. Population of the Scattered Kuiper Belt *Ap. J.* **102**, 529–533.

Wisdom, J. 1980. The resonance overlap criterion and the onset of stochastic behavior in the restricted three-body problem. *Astron. J* **85**, 1122-1133.

Wisdom, J., Holman, M. 1991. Symplectic maps for the n-body problem. *A. J.* **102**, 1528–1538.

Table 1. Astrometric observations for 2000 CR_{105}

Object	UT Date yyyy mm dd.ddddd	α(2000) hh mm ss.ss	δ (2000) dd mm ss.s	R mag	Obs. Code	Note
K00CA5R	2000 02 06.30637	09 14 02.39	+19 05 58.7	22.5 R	695	1
K00CA5R	2000 02 06.43541	09 14 01.90	+19 06 01.4		695	1
K00CA5R	2000 02 27.12907	09 12 44.37	+19 13 04.6	23.0 R	695	1
K00CA5R	2000 02 27.22612	09 12 43.98	+19 13 06.3		695	1
K00CA5R	2000 03 28.38346	09 11 17.68	+19 20 37.4		568	2
K00CA5R	2000 03 28.40927	09 11 17.63	+19 20 37.6		568	2
K00CA5R	2000 03 28.43164	09 11 17.59	+19 20 37.9		568	2
K00CA5R	2000 03 29.23055	09 11 15.99	+19 20 46.3		568	2
K00CA5R	2000 03 29.25196	09 11 15.95	+19 20 46.5	23.1 R	568	2
K00CA5R	2000 03 29.27248	09 11 15.91	+19 20 46.7	23.4 R	568	2
K00CA5R	2000 11 24.30080	09 22 07.39	+18 49 14.6		809	3 *
K00CA5R	2000 11 25.30941	09 22 06.97	+18 49 25.1		809	3 *
K00CA5R	2000 11 27.48283	09 22 05.77	+18 49 49.1	23.5 R	675	4
K00CA5R	2000 11 27.54557	09 22 05.73	+18 49 49.1	23.7 R	675	4
K00CA5R	2000 11 28.48968	09 22 05.11	+18 49 59.8	24.1 R	675	4
K00CA5R	2000 11 28.52381	09 22 05.08	+18 50 00.3	23.6 R	675	4
K00CA5R	2000 12 17.45692	09 21 38.68	+18 54 34.5	23.0 R	695	5
K00CA5R	2000 12 17.49240	09 21 38.62	+18 54 34.9	23.2 R	695	5
K00CA5R	2000 12 17.53331	09 21 38.54	+18 54 35.9	23.4 R	695	5
K00CA5R	2000 12 18.43274	09 21 36.63	+18 54 51.1	23.0 R	695	5
K00CA5R	2000 12 18.50613	09 21 36.52	+18 54 52.2	22.8 R	695	5 *
K00CA5R	2001 01 20.39079	09 19 58.51	+19 06 04.4	23.1 R	675	6
K00CA5R	2001 01 20.39910	09 19 58.46	+19 06 04.6		675	6
K00CA5R	2001 01 20.46716	09 19 58.24	+19 06 06.2	23.1 R	675	6
K00CA5R	2001 02 15.99209	09 18 17.96	+19 15 46.4	23.7 R	950	7
K00CA5R	2001 02 16.03317	09 18 17.80	+19 15 47.2	23.4 R	950	7
K00CA5R	2001 02 16.08746	09 18 17.59	+19 15 48.4	23.5 R	950	7
K00CA5R	2001 02 23.15703	09 17 51.48	+19 18 11.2	23.3 R	309	8
K00CA5R	2001 02 24.24770	09 17 47.52	+19 18 32.4		309	8
K00CA5R	2001 03 29.14814	09 16 11.17	+19 26 53.5	23.5 R	695	9
K00CA5R	2001 03 30.14350	09 16 09.16	+19 27 03.6		695	9
K00CA5R	2001 03 31.13533	09 16 07.21	+19 27 13.8	23.5 R	695	9
K00CA5R	2001 12 12.15628	09 26 35.96	+18 58 23.1		950	10
K00CA5R	2001 12 12.19915	09 26 35.90	+18 58 23.8		950	10
K00CA5R	2001 12 12.23953	09 26 35.84	+18 58 24.5	23.4 R	950	10
K00CA5R	2001 12 13.16493	09 26 34.33	+18 58 39.2	23.4 R	950	10
K00CA5R	2001 12 13.20038	09 26 34.28	+18 58 39.7		950	10

Notes: 1 – Millis *et al.* KPNO 4-m and WIYN (MPEC 2000-F07)
2 – Gladman, Kavelaars, Holman, Petit (CFHT-3.5m); 3 – Gladman (ESO-2.2m);
4 – Nicholson, Kavelaars (Palomar-5m); 5 – Holman, Gladman, Grav (KPNO-4m);
6 – Nicholson, Gladman (Palomar-5m); 7 – Grav, Holman (NOT-2.5m);
8 – Gladman (VLT UT1-8m); 9 – Gladman, Davis, Neese (KPNO 4-m);
10 – Grav (NOT-2.5m)

Astrometric uncertainties $\alpha \pm 0.03s$, $\delta \pm 0.4''$ except $*$ for which $\alpha \pm 0.07s$, $\delta \pm 1''$.
Photometric uncertainties $\pm$ 0.5 mag

Table 2. Barycentric orbital elements for 2000 CR_{105} (Epoch: JD 2451580.8)

Orbital element (J2000)	Value	1-sigma error
semimajor axis a	221 AU	1 AU
eccentricity e	0.800	0.001
perihelion distance q	44.14	0.02 AU
inclination i	22.758°	0.001°
longitude of node Ω	128.286°	0.001°
argument of pericenter ω	316.72°	0.06°
Date of pericenter passage (JD)	2438857	5
mean anomaly M	3.83°	0.03°

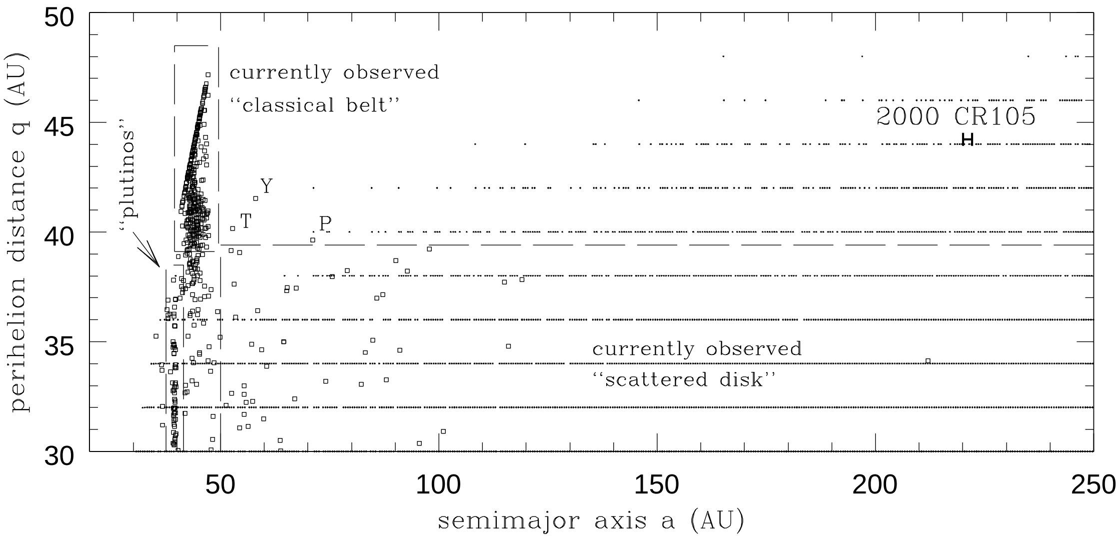

Figure 1: Open squares indicate estimated semimajor axes and perihelion distances for all trans-neptunian objects in the Minor Planet Center database as of January 10 2002. Very approximate boundaries for membership in the classical Kuiper Belt, plutino population, and scattered disk are indicated (only to guide the eye). An error bar is shown for the orbit of 2000 CR_{105}, and the TNOs current orbital elements of 1995 TL_8, 2000 PH_{30}, and 2000 YW_{134} are indicated by the points labelled T, P, and Y, respectively. Small points indicate that a numerical integration (see text) showed a chaotic orbital evolution for an orbit with those initial conditions. Note that there are severe detection biases in this plot and it is not a representative sampling of the trans-neptunian region.

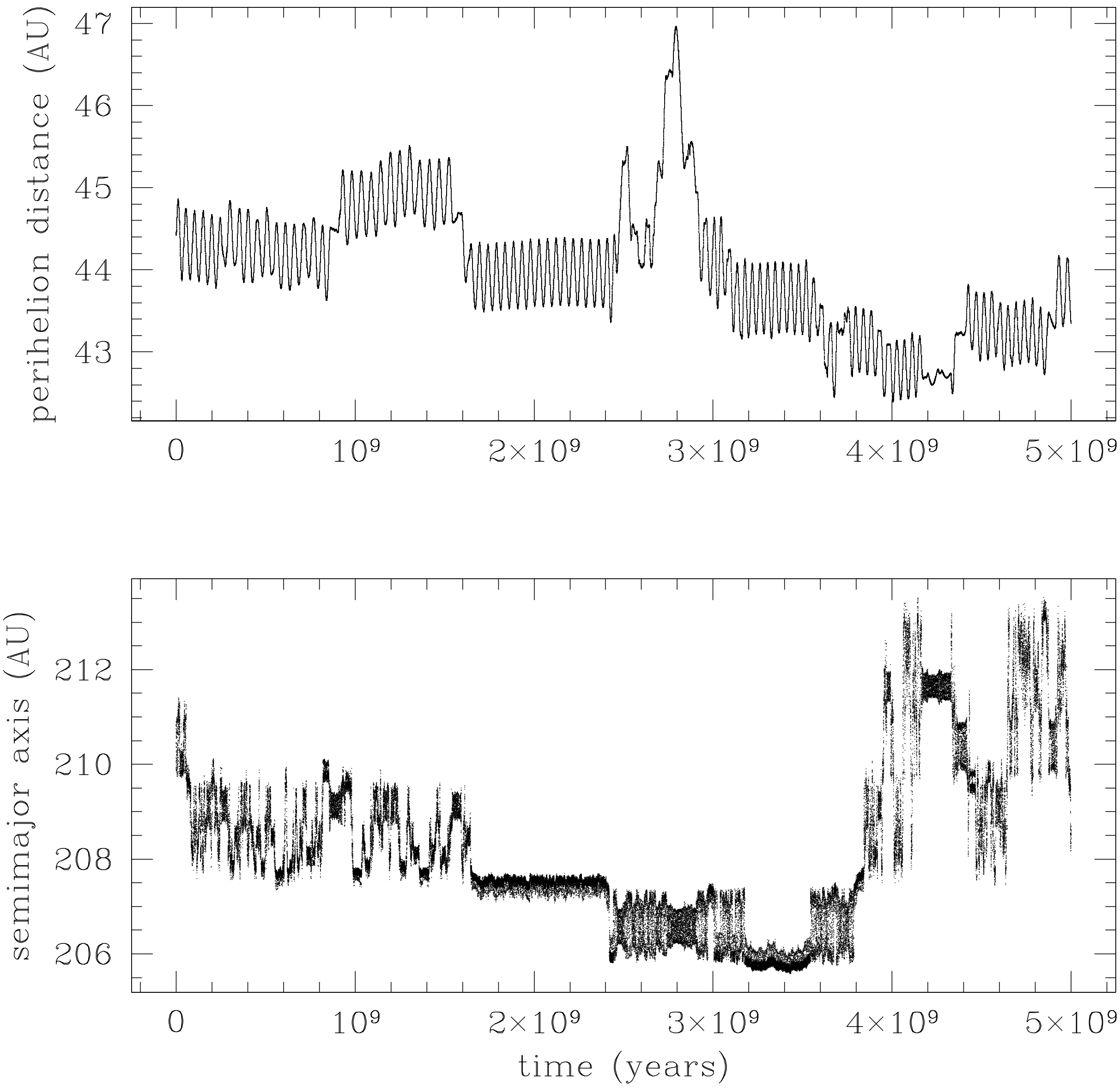

Figure 2: The evolution for the semimajor axis a and pericentric distance q for a test particle integrated with an initial orbit consistent with that of 2000 CR_{105}. The plotted orbital elements are barycentric. See text for discussion.

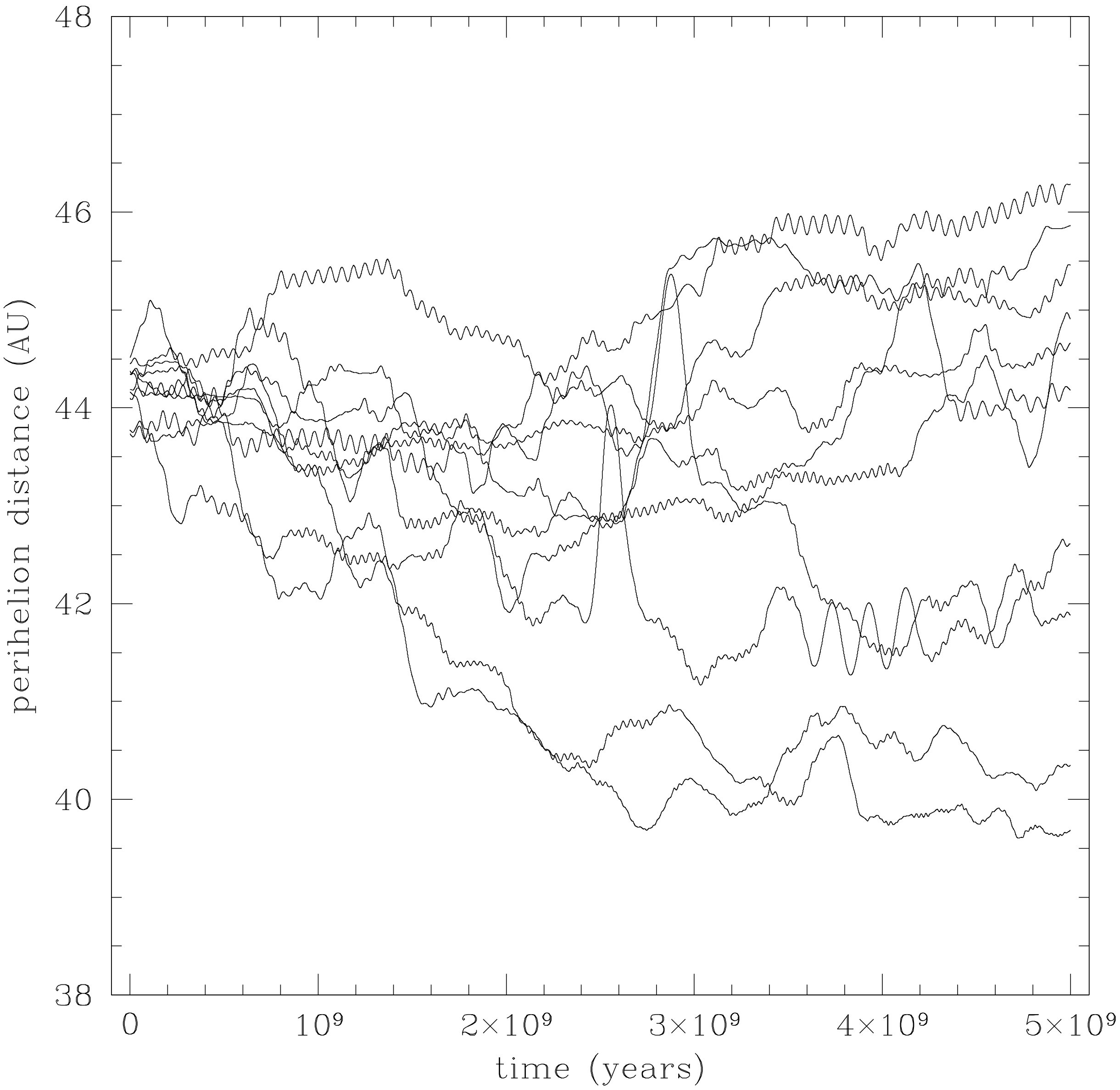

Figure 3: The q-evolution for 10 of the 20 integrated 'clones', showing the range of variation for particles consistent with the fitted orbit of 2000 CR_{105}. The remaining 10 particles fell within the bounds shown by these evolutions.

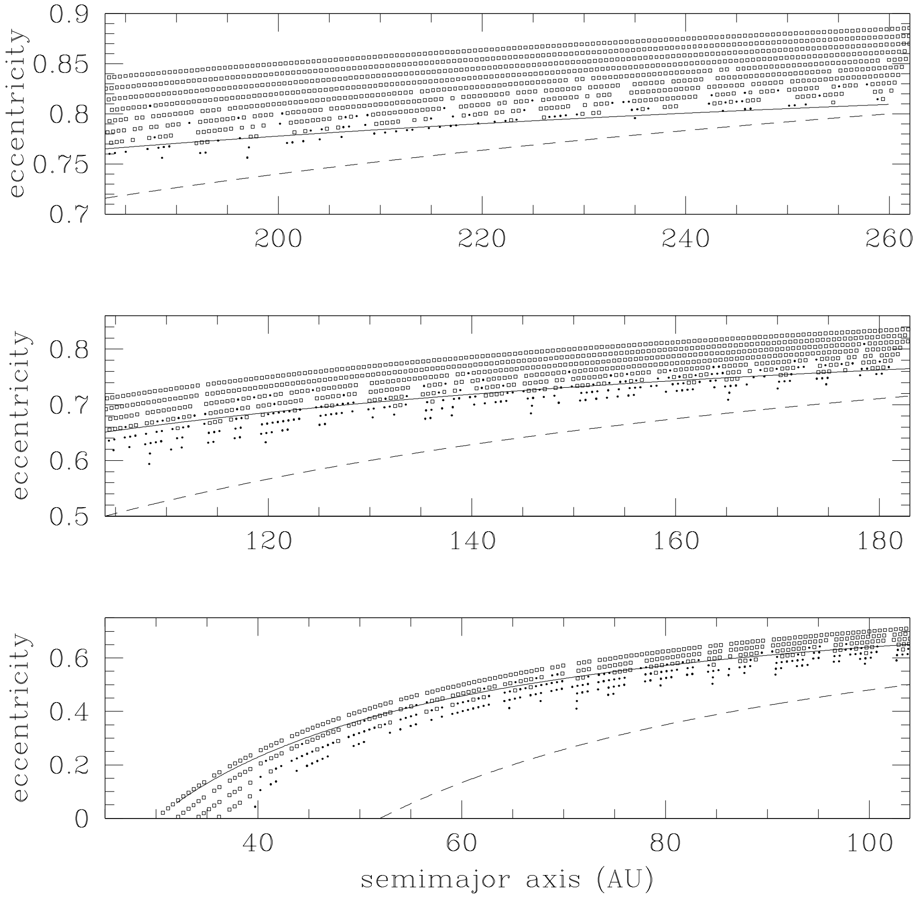

Figure 4: An illustration of the chaotic structure of the region of large-a solar system orbits. Initial conditions correspond to heliocentric orbits with a=30–260 AU and e selected to sample q=30–52 AU in increments of 2 AU. For the remaining elements we chose inclination $i = 17°$, longitude of ascending node $\Omega = 0°$, argument of perihelion $\omega = 0°$, and mean anomaly $M = 0°$, with respect to the DE403 ecliptic and equinox. Each open square corresponds to an integrated trajectory (see text) with Lyapunov time shorter than 20 of its orbital periods; small dots correpond to Lyapunov times less than 100,000 years. The solid line denotes the relation $q = 30 + 0.085(a - 30)$ (determined empirically) which roughly bounds the envelope of trajectories chaotic on the orbital period time scale. Above this line, most of the trajectories exhibit strong, short time-scale chaos. The dashed line denotes the lower eccentricity boundary of the integrated trajectories (q=52 AU). Between the dashed line and the solid line most of the trajectories that exhibit chaos due so only on time scales much longer than their orbital periods. The 'fingers' of regular regions at large a (absence of points), reaching to higher values of e, correspond to the stable regions associated with individual mean-motion resonances.

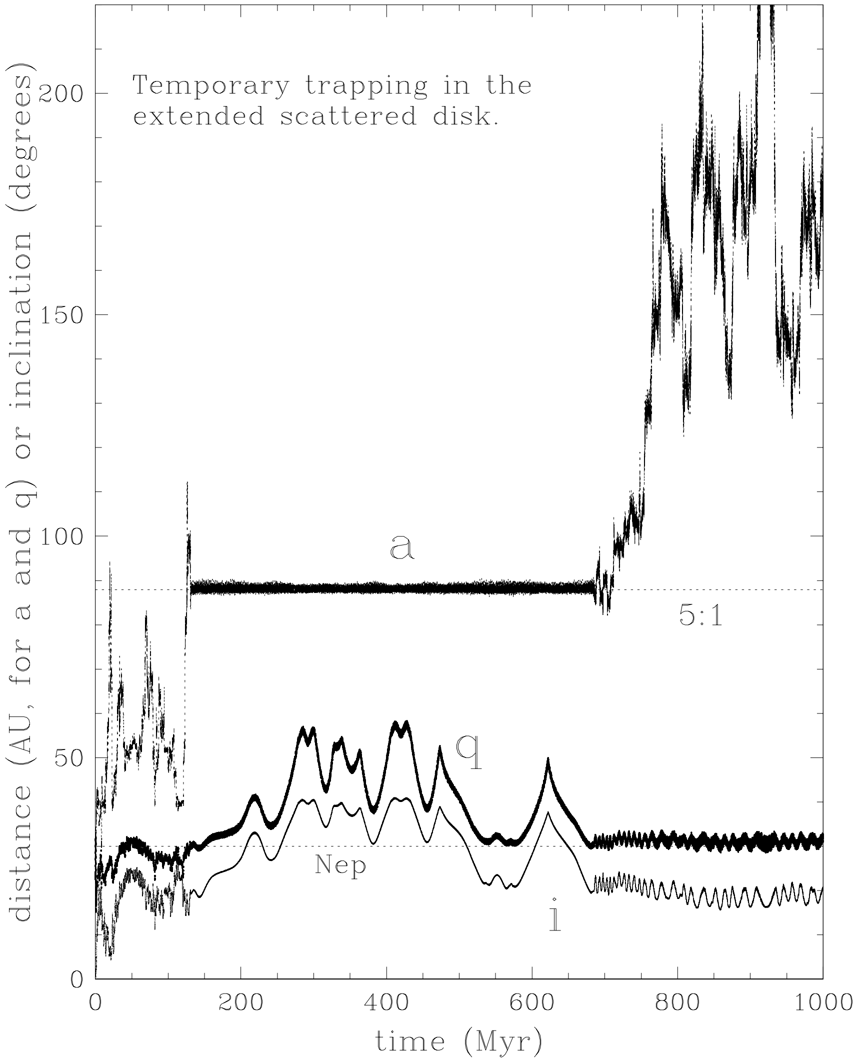

Figure 5: An example of temporary trapping in the extended scattered disk. The test particle began on circular orbit with a=32 AU and zero inclination. After an initial stage of about 130 Myr in the scattered disk with perihelion very near or interior to Neptune, the semimajor axis lands near that of the 5:1 mean-motion resonance with Neptune at $a \simeq$88 AU. Due to the influence of the resonance, the perihelion q rises very far above 30 AU; the fact that while in the resonance the evolution of the inclination i and q are strongly correlated indicates that the Kozai resonance is present inside the mean-motion resoance. After more than 500 Myr in the resonance a strong interaction with Neptune removes the particle from the resonance. This temporary 'resonant decoupling' is commonly seen inside the 2:1 resonance (about 0.5% of all initial conditions temporarily have q >37 AU while inside the resonance), rarely from a=50-100 AU ($\sim$0.1% have q >37 AU while in some mean-motion resonances with Neptune), and never seen (no cases in our integrations) for a >100 AU.

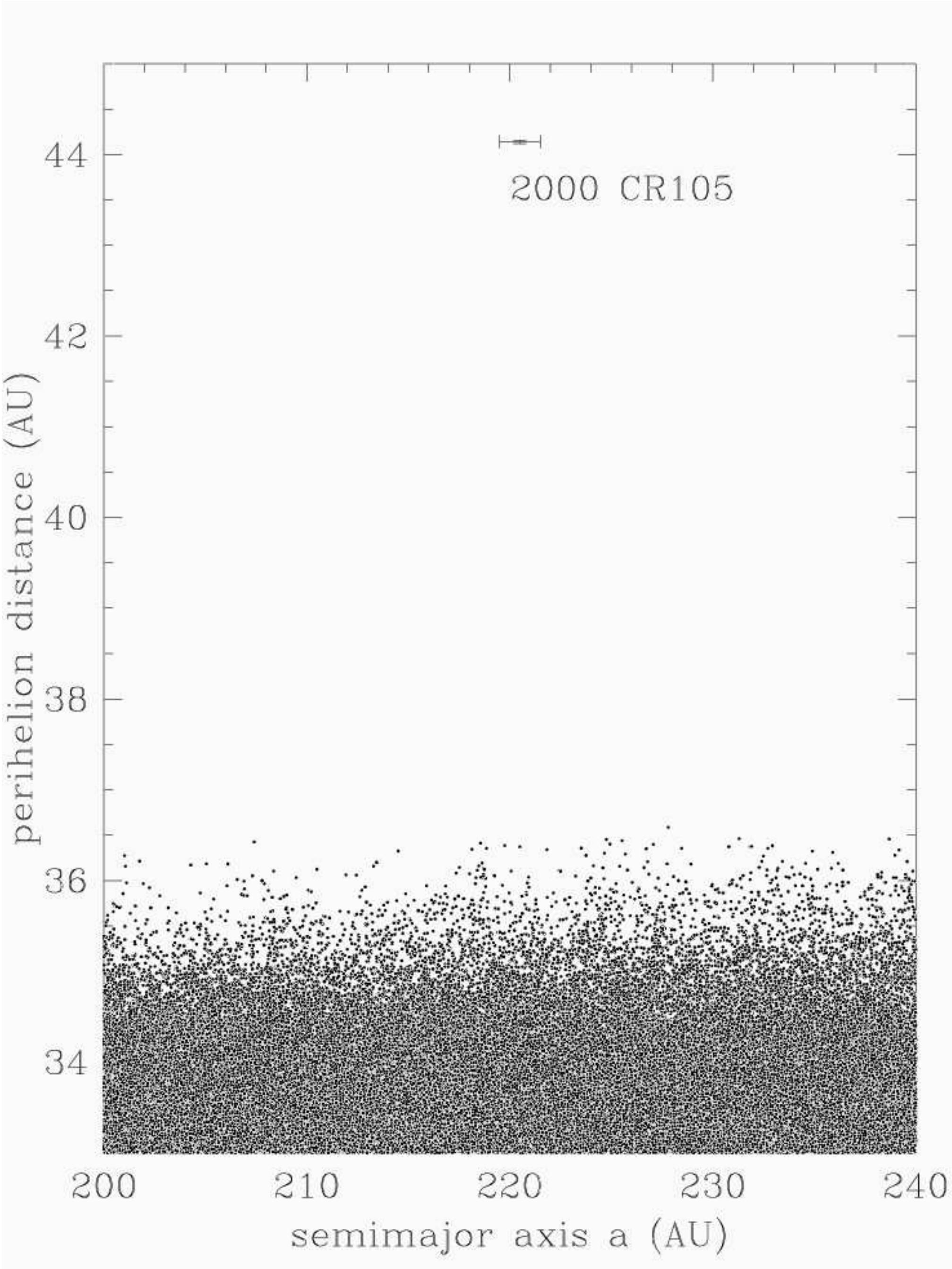

Figure 6: A comparison of the orbital elements of 2000 CR_{105} with those explored by our integrations. The error bar indicates the estimated orbital position of 2000 CR_{105} at the 1-sigma level. Our numerical simulations were sampled at 10^4 yr intervals, and a point on this plot indicates that an integrated particle had the corresponding orbital elements at that time (and thus, the density of points is proportional to the fraction of a steady-state population with those elements).